IEEE Access
Multidisciplinary | Rapid Review | Open Access Journal

Received September 27, 2018, accepted October 12, 2018, date of publication October 24, 2018,
date of current version November 19, 2018.

Digital Object Identifier 10.1109/ACCESS.2018.2877887

Pulse Compressed Time Domain Multiplexed Fiber Bragg Grating Sensor: A Comparative Study

M. M. ELGAUD[1], AHMAD ASHRIF A. BAKAR[1], (Senior Member, IEEE), ABDULFATAH ABUSHAGUR GHAITH[1], NANI FADZLINA NAIM[2], NORHANA ARSAD[1], (Member, IEEE), MOHD HADRI HAFIZ MOKHTAR[1], (Member, IEEE), NUR HIDAYAH AZEMAN[1], AND MOHD SAIFUL DZULKEFLY ZAN[1], (Member, IEEE)

[1]Center of Advanced Electronic and Communication Engineering, Faculty of Engineering and Built Environment, Universiti Kebangsaan Malaysia, Bangi 43600, Malaysia

[2]Faculty of Electrical Engineering, Universiti Teknologi MARA, Shah Alam 40000, Malaysia

Corresponding authors: Ahmad Ashrif A. Bakar (ashrif@ukm.edu.my) and Mohd Saiful Dzulkefly Zan (saifuldzul@ukm.edu.my)

This work was supported in part by the Ministry of Higher Education Malaysia under Grant FRGS/1/2016/TK04/UKM/02/7 and in part by the Faculty of Engineering and Built Environment, UKM, under Grant DIP-2017-003.

ABSTRACT This paper experimentally demonstrates the feasibility of improving the sensing performance of fiber Bragg grating (FBG)-based point sensors by deploying two pulse coding techniques, simplex coding (SSC), and Golay complementary codes (GCC). The two techniques are separately combined with the conventional time-domain multiplexed FBG (TDM-FBG) interrogation sensor, and their results are compared with respect to the conventional single pulse interrogation technique. Consistently with the theory, for both the coding techniques, we have confirmed that the signal-to-noise ratio improved proportionally to the code length. In details, for both the techniques, the signal-to-noise improvement ratio of two FBGs located after around 16.35 km of fiber has significantly increased up to about 6 dB. Furthermore, the decoded signals from both techniques conserve their original spatial properties, confirming the successfulness of Hadamard transform and Golay auto-correlation calculations. Our experimental analysis confirms the simplex codes with their significant noise reduction ability, which is translated into well formed and accurate mean amplitude calculations. Moreover, the analysis of TDM-FBG-based GCCs have confirmed the unique properties of the auto-correlation process to increase the FBG signals up to around 128 times compared with the single pulse case.

INDEX TERMS TDM-FBG, signal-to-noise-ratio, Golay complementary codes (GCC), auto-correlation, simplex pulse coding, SSC, Hadamard transform, Noise reduction.

I. INTRODUCTION

Optical fiber sensors (OFS) have been deployed widely for a variety of physical measurands such as temperature, strain, pressure, and vibration [1]–[3]. In the field of distributed sensing, where a dense distribution is needed to sense at a specific location, fiber Bragg grating (FBG) sensors considered as an effective sensing element [4], [5]. Their simplicity in multiplexing and embedding capabilities, lightweight, immunity to the electromagnetic distortions and ease of installation, making them a suitable choice in wide range of deployments including structural health monitoring, pipeline leakage detection, and building security systems [4]–[8]. Time domain multiplexing (TDM) and wave division multiplexing (WDM) have been the common FBG multiplexing techniques reported recently [8].

In WDM system, the network capacity is limited by the ratio of optical source spectral width over the dynamic range of FBG sensor. Thus, the number of FBG sensors that can be employed in WDM is restricted to few tens only [8]. On the other hand, TDM systems can multiplex few hundreds to a thousand sensing points if the cross-talk levels between the adjacent sensors are carefully determined [9], [10]. However, traditional TDM-FBG systems with large-scale deployments still suffer from low signal-to-noise ratio (SNR), limited measurement range and distance. Improving the SNR of the FBG signals is possible by increasing the input power or the pulse duration of the pulsed light injected into the sensing area. Nonetheless, excessively high power will severely degrade the overall system performance due to nonlinear scatterings such as Raman and Brillouin, while increasing the pulse

duration reduces the spatial resolution and the multiplexing ability [7]–[11]. Conventional SNR improvement methods such as accumulative averages would reduce the measurement speed [16], [19].

In this context, pulse compression technique is found to be an effective method to improve the SNR without increasing the input power or impairing the system spatial characteristics. In addition, the technique improves the trade-off between the pulsed light duration and the distance between adjacent sensing points. The technique provides the interrogation light with sufficient energy by encoding it over wide sequences consist of multiple narrow pulses [11], [15]. During the decoding process, the received wide signal is compressed to narrow pulse according to the decoding algorithm. There is a considerable amount of literature reports on the enhancement of distributed optical fiber (DOF) sensors by employing compressed sequences such as Golay complementary codes (GCC), dual GCCs, Walsh, simplex and combined Walsh/GCC codes [11]–[15].

However, as the abovementioned works mainly focus on the DOF field, little attention has been paid to apply the variety of pulse compression technique to quasi-distributed sensors such as TDM-FBG sensors. Although the deployment of cyclic S-codes and GCC in TDM-FBGs have been reported recently, the literature of those two common techniques still has not been well grounded [11], [15]. In addition to the absence of the experimental validation of Golay coded TDM-FBGs, there is still a need to provide a comparative study that illustrates the strength and weakness of both GCC and the standard simplex code (SSC).

Therefore, in this paper, we extensively investigated the performance of TDM-FBG sensor under two pulse coding techniques, SSC and GCC. The performance parameters of the two techniques were compared with the conventional single pulse interrogation technique. From the experimental analysis, conventionally interrogating two identical low reflectivity FBG sensors spliced at the end of about 16.35 km single-mode fiber (SMF) has resulted the poorest FBG signals in terms of SNR, signal strength and the pulse shape. Under the same condition, the deployment of SSC and GCC up to 63 and 64 bits respectively, have significantly improved the SNR of the two FBG signals up to about 6 dB. Consistently with the theory, the decoding of the FBG pulses by both techniques has confirmed correct Hadamard transform and Golay autocorrelation calculations. Moreover, their SNR has improved proportionally with the codelength without impacting the system spatial properties. The results confirmed the GCC deployment capabilities to provide the decoded FBG signals with the amplitude increment that guarantees better FBG bandwidth utilization at short processing time.

On the other hand, simplex coded FBG signals confirmed better pulse shapes and well-formed edges compared to the GCC deployment but with longer processing time and more complex approach. In our previous works, we have successfully demonstrated for the first time, the simulations of designing and implementing Golay coded TDM-FBG technique [15]. To the best of our knowledge, the experimental demonstration of Golay coded TDM-FBG has never been explored.

II. FUNDAMENTALS OF PULSE COMPRESSED TDM-FBGs

FBG sensors are known as a promising high sensitivity sensing element. FBG uses the Bragg wavelength shift ($\Delta\lambda$) induced by the physical effect applied to the sensor to indicate the measured quantity. The relationship between the wavelength shift induced by the temperature or the strain effect can be expressed as:

$$\Delta\lambda B = (\alpha + \beta)\Delta T + (1 - pe)\varepsilon \tag{1}$$

Where α and β are the fiber thermal expansion and the thermo-optic coefficients respectively, pe is the fiber material photo-elastic coefficient. T and ε are the temperature and the strain applied to the FBG [1]–[3].

A. CONVENTIONAL SINGLE PULSE TDM-FBG SENSING ARRAY

Figure 1 schematically illustrates the standard TDM-FBG sensing array. A continuous wave (CW) laser with an extremely narrow line width intensity modulated over a single pulse with sufficient width and energy. The pulsed light is used to interrogate a set of identical broadband and low reflectivity FBGs planted on the locations to be monitored [8]–[11], [15].

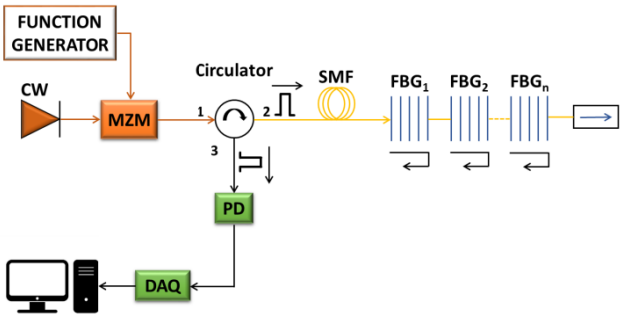

CW = Continuous wave; MZM = Mach-Zehnder modulator; SMF = Single mode fiber; PD = Photo detector; DAQ = Data acquisition.

FIGURE 1. Standard TDM-FBG system.

Since the FBGs have low reflectivity and serially connected, the pulse continuously flows from each FBG to the next. The multiple reflected FBG signals are channeled to the receiver section via port 3 of the circulator, where they are being distinguishable based on their time of arrivals. Since the reflectivity profile of each FBG is shifted linearly with respect to the physical effect applied, the result of any changes made to the FBGs will appear as an amplitude variation on the time domain traces of their reflected pulses [11], [15].

B. SIMPLEX CODED TDM-FBG SENSING ARRAY

In this method, the key technique to improve the SNR system is to modulate the interrogation light over a series of pulses

encoded corresponding to S-matrix. S-matrix is a unipolar matrix of ones and zeros, the rows of this matrix are called simplex codes. S-matrix of the length M codes can be derived by omitting the rows and column of the bipolar Hadamard matrix of $M+1$ size and replace each -1 by 1. The calculations include the use of simplex codes or Hadamard matrix, which are defined as Hadamard transform.

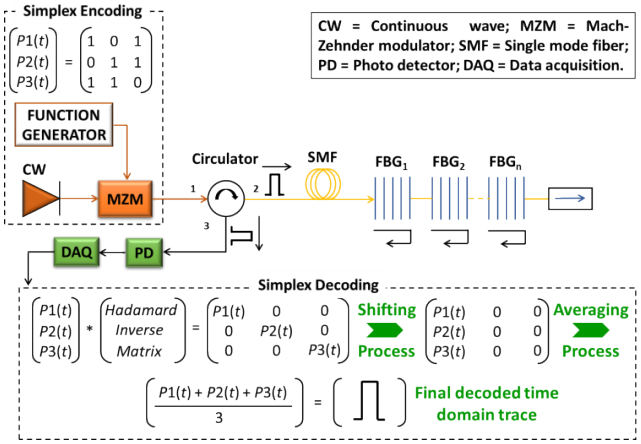

FIGURE 2. Simplex coded TDM-FBG involving Hadamard transform calculations for 3 bits case.

Figure 2 illustrates the physical realization of the coded TDM-FBG equivalent to order 3 of S-matrix. At the encoding section, the total number of three traces are injected to the sensing area one by one, their responses are directed to the receiver section via port 3 of the circulator and arranged in $M = 3$ sized matrix. At the decoding section, to recover the original traces, the matrix contained of the reflected FBG signals are then multiplied by the inverse of bipolar Hadamard matrix [16], [17].

The outcomes of this process are aligned and shifted with respect to the first time domain trace and averaged. The final trace of this process exhibits the exact spatial properties of the original single pulse signal. To quantify the signal-to-noise improvement ratio (SNIR), the SNR of the decoded trace should be compared to the one obtained by the trace averaged conventionally 3 times, as in (2):

$$SNIR_{S\ coded\ (3bits)} = \frac{SNIR_{S\ coded\ (3bits)}}{SNIR_{S\ Averged\ (3\ times)}} \tag{2}$$

Assuming the system with zero mean uncorrelated noise of σ^2 variance, then the noise reduction provided by 3 bits SSC equals to $\sigma^2/4$. Since the noise reduction provided by conventionally averaging three identical single pulse time domain traces is $\sigma^2/3$, then the SNIR by deploying 3 bits SSC can be obtained by comparing the two quantities, as follows:

$$SNIR_{S\ coded\ (3bits)} = \sqrt{\frac{\sigma^2/3}{\sigma^2/4}} = \sqrt{\frac{4}{3}} = \frac{2}{\sqrt{3}} \tag{3}$$

In general, the SNIR of M bits SSC can be defined as [16], [17]:

$$SNIR_{S\ coded\ (M bits)} = \frac{M+1}{2\sqrt{M}} \tag{4}$$

C. GOLAY CODED TDM-FBG SENSING ARRAY

Golay code is a binary pair of codes A and B with same code length L, with their auto-correlation functions having the same main lobe sign and amplitude, and opposite side lobes signs. Summation of both autocorrelations gives the perfect autocorrelation function i.e., doubled amplitude of main lobe with cancelled side lobes. Mathematically, the concept of GCC autocorrelation calculations can be expressed as follows [12], [13], [15]:

$$\emptyset_{A,A}(k) + \emptyset_{B,B}(k) = 2L\delta(k) \tag{5}$$

where;

$$\emptyset_{A,A}(k) = \sum_{m=0}^{L-k-1} a_{(m+k)}a_m \tag{6}$$

$$\emptyset_{B,B}(k) = \sum_{m=0}^{L-k-1} b_{(m+k)}b_m \tag{7}$$

and:

$$\delta(k) = \begin{cases} 1, & for\ k = 0 \\ 0, & elsewhere \end{cases}$$

In the equation above, L represents the code lengths of A and B sequences and k is the bit shifting during the autocorrelation process. Golay pairs can be recursively generated as in $\{[AB]; [A(-B)]\}$. For example, for a given pair of $\{A = 1; B = 1\}$, the next Golay pair that can be constructed is $\{[1\ 1]; [1\ -1]\}$ for 2 bits case, and $\{[1\ 1\ 1\ -1]; [1\ 1\ -1\ 1]\}$ for 4 bits case [15], [18], [19].

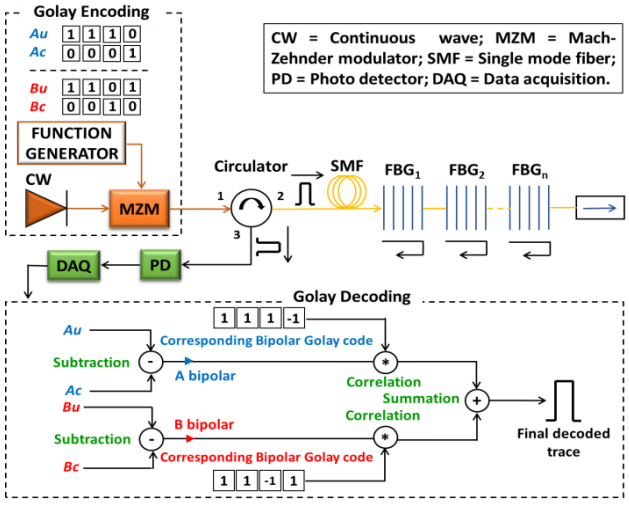

FIGURE 3. Golay coded TDM-FBG involving 4 bits GCC deployment.

However, it should be noted that Golay pairs are originally bipolar codes. To achieve Golay coded TDM-FBG based on direct detection, the unipolar form of GCC should be introduced. Figure 3 depicts the concept of encoding

standard TDM-FBG with 4 bits unipolar GCC [19], [20]. In the encoding section, the bipolar Golay pair is reformed into four unipolar codes by introducing the unipolar form of each pair followed by its ones complement as in $\{(A_u, A_c); (B_u, B_c)\}$. The four unipolar codes are injected to the sensing area one by one and each of their responses is acquired and stored. At the decoding section, the signal response of *Au* is subtracted from *Ac* and that of *Bu* from *Bc*. The resulted codes are then correlated with their corresponding bipolar GCC and finally summed up to give the final measurement signal [19].

Extending GCC length to the next one builds up the decoded signal amplitude proportionally to L, at the same time the noise grows on root mean square values of L. Hence, the SNIR of the system can be expressed as:

$$SINR_{Bipolar} = \frac{L}{\sqrt{L}} = \sqrt{L} \tag{8}$$

Since the deployment of unipolar GCC requires four traces, SNIR values equal to half of that obtained by the bipolar case, as follows:

$$SINR_{Unipolar} = \frac{SINR_{Bipolar}}{2} = \frac{\sqrt{L}}{2} \tag{9}$$

In comparison with the 4 bits GCC case, the maximum value of 6.05 dB SNIR can be obtained when deploying 64 bits unipolar GCCs, as in $SNIR = (10Log16/\sqrt{16})$ [18]–[20].

III. EXPERIMENTAL SETUP

Figure 4 shows the experimental setup of TDM-FBG sensor employing SSC and GCC. A narrow CW laser source with 1548.62nm center wavelength and 8 dBm power was connected to an intensity modulator of Mach-Zehnder (MZM) type. The modulator was driven by an arbitrary wave generator (AWG) of 10 ns width NRZ pulses at 1 Gs/s sampling rate. The AWG transmission setting was based on the application on duty, whether generating the conventional single pulse or stream of coded sequences. The modulated pulses were then amplified by an Erbium-doped optical amplifier (EDFA) and launched to the sensing area via the port 2 of the optical circulator. The sensing area consisted of two identical FBGs were spliced to the end of around 16.35 km SMF spool. The two FBGs were spatially separated by around 5 m. Their bandwidth, reflectivity and center wavelength were 2.5 nm, 2.5 % and 1550.2 nm respectively. The FBG signals reflected back from the sensing area were routed to the receiver section via port 3 of the circulator. The receiver section consisted of high-speed photo-detector and digital signal processing unit for data acquisitions and analysis. The experiment was carried out at the room temperature, while the measurement condition such as the input power remained constant during the entire experiment. The conventional single pulse interrogation session was carried out first, followed by the SSC and then GCC. It should be noted that the spatial characteristics of the decoded pulses during the deployments of SSC and GCC were compared to those obtained by the conventional single pulse technique.

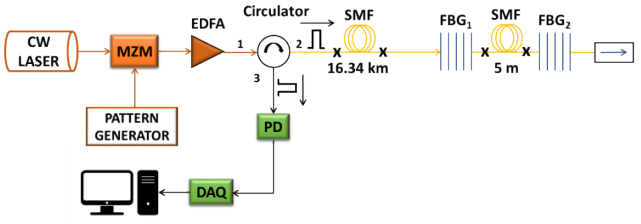

CW = Continuous wave; MZM = Mach-Zehnder modulator; EDFA = Erbium-Doped Fiber Amplifier; SMF = Single mode fiber; PD = Photo detector; DAQ = Data acquisition.

FIGURE 4. Schematic setup of coded TDM-FBG sensing array.

IV. RESULTS

This section illustrates the impact of the interrogation technique to the performance parameters of TDM-FBG sensor such as decoded signal shape, noise behavior and SNR. The impact of deploying the conventional single pulse technique is presented separately in the first section, followed by that of SSC and GCC.

A. DEPLOYMENT OF CONVENTIONAL TDM-FBG TECHNIQUE

Figure 5 shows the FBG signals measured by the conventional single pulse technique. To detect the FBG locations and spatial properties, the single shot time domain trace acquired by the oscilloscope was translated into a distance scale by using the approximation factor of 10 ns = 1 m. Figure 5 depicts the distorted pulses with large noise background and low SNR for both FBG signals. These drawbacks limit the large scale of TDM-FBG deployments and have led the researchers to carry out pulse coding techniques to provide better overall performance.

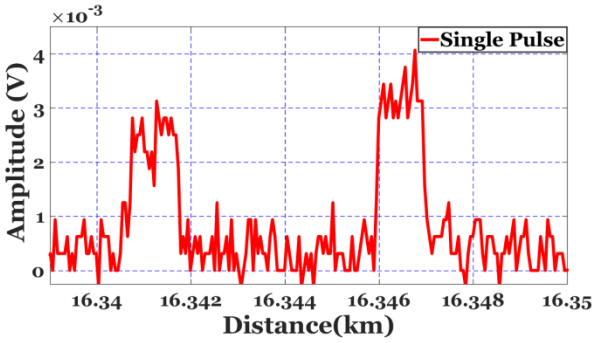

FIGURE 5. FBG signals response to conventional single pulse interrogation.

B. CODED TDM-FBG SENSING ARRAY

In this section, the effect of increasing the code lengths on the FBG signals was analyzed. For the sake of fair comparison, the total numbers of five code iterations were conducted corresponding to each technique. The setup firstly interrogated by the deployment of 3, 7, 15, 31 and 63 bits of SSC, followed by the GCC of code lengths 4, 8, 16, 32 and 64 bits.

1) EFFECT OF THE CODE LENGTH TO THE FBG SIGNAL RESPONSE

In this section, we analyzed the effect of multiple code lengths of SSC and GCC to the FBG signal shape, amplitude and spatial characteristics. Figures 6(a) and (b) compare the FBG signal response to the deployment of 3, 7, 15, 31 and 63 bits of SSC, and of 4, 8, 16, 32 and 64 of GCC respectively. As observed from Figs. 6, for both SSC and GCC techniques, the FBG pulses decoded at all code lengths conserve the spatial properties of the original single pulse presented in Fig. 5, indicating the successful Hadamard transform and Golay auto-correlation procedure without impairing the location accuracy of the FBGs. In the case of SSC deployment, as depicted in Fig. 6(a), both of the pulse shape and the noise background have been gradually improved with every increase in the code-length, reaching their best at 63 bits; this indicates better measurement accuracy, precision, and high SNR. It is worth to mention that, for any code length, SSC deployment did not increase the FBG signals amplitudes due to the averaging during the decoding. However, it should be noted that at the same time, the random noise has also reduced significantly.

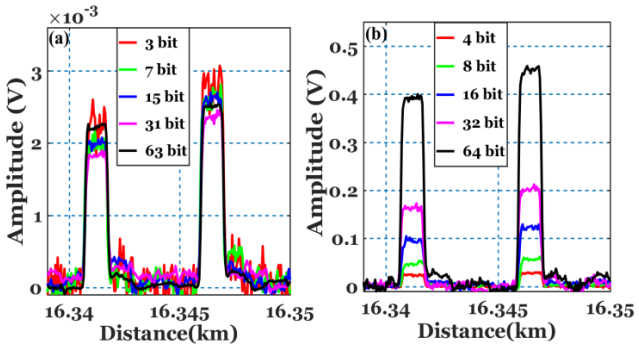

FIGURE 6. FBG signals response to increasing code length for (a) SSC and (b) GCC deployments.

On the other hand, the deployment of GCC illustrates a completely different case. The amplitude of the decoded FBG signals increased linearly with the code length L; this theoretically agrees with that explained in Section II. Figure 6(b) illustrates the proportional increase of the FBG signals amplitudes with respect to the application of 4, 8, 16, 32 and 64 bits of GCC. The signal strength at this point is 128 times higher than the single pulse and SSC case.

2) EFFECT OF THE CODE LENGTH TO THE SYSTEM NOISE AMPLITUDE

In this section, the impact of increasing the code length to the system noise was numerically analyzed. The noise amplitude for both techniques was quantified by the standard deviation along 318100 points of data on the time domain trace of each decoded pulse.

Figure 7(a) illustrates the system noise as a function of SSC code lengths. Considering the single pulse case as a reference, the deployment of SSC with M bits length has reduced the noise with $2/(M+1)$ factor. The measured data continues decreasing linearly with the increase in code length, reaching its optimum at the 63 bits case. In an excellent agreement with the theory, the system noise at this point has improved by 31.5 times compared to that of conventional single pulse technique.

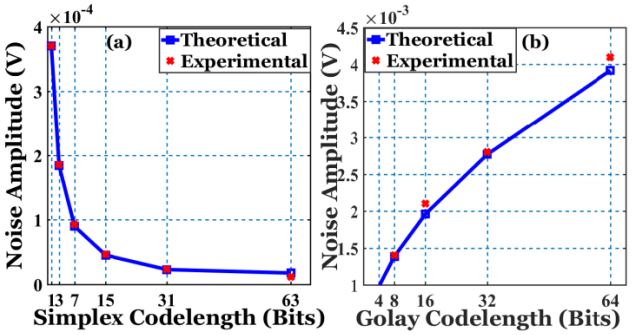

FIGURE 7. TDM-FBG response as a function of code lengths for (a) SSC and (b) GCC deployments.

However, the system noise behaves differently during the deployment of GCC codes. In fact, the system noise does increase with respect to the extending of GCC code lengths applied. As mentioned in section II(C), during the auto-correlations of GCC, the attended uncorrelated Gaussian distributed noise grows on mean square roots. Figure 7(b) illustrates the noise growth as a function of the code length.

In line with the theory, our experimental analysis shows that the noise builds up by the factor of $\sqrt{2}$ with respect to each step up than 4 bits length. Further analysis regarding the noise contribution to the SNR of the FBG signals for both techniques is discussed in the next section.

3) EFFECT OF THE CODE LENGTH TO THE SNR

In this section, we investigated the SNIR contributed from the deployment of the two coding techniques. The SNR of the decoded pulses was calculated by dividing the mean amplitude with the standard deviation of the random noise.

In the case of SSC, the SNR for each decoded signal at M bits was compared to the SNR associated to the conventional single pulse measurement averaged M times. Fig. 8(a) illustrates the SNIR curve as a function of code length up to $M = 63$ bit. The theoretical curve was plotted with respect to (4). The curve illustrates consistent results with the theory for both FBGs up to $M = 31$ bit. When $M = 63$ bits, due to some acquisition error during retrieving the experimental data needed for averaging, the SNIR values were higher than the theoretical.

In the case of GCC, the SNR associated to each code length was divided by that of SNR of 4 bits case and plotted as a function of the code length. Further analysis and insights can be illustrated on the light of (9). Considering the 4 bits case as reference, each step toward the next code provides the FBG signals with a peak increment of the factor 2. Meanwhile, the noise builds up by the factor of $\sqrt{2}$. In other words, the system SNR increases with the value of about 1.5 dB

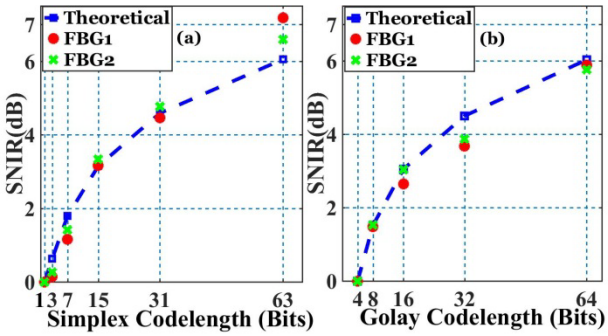

FIGURE 8. SNIR curves as a function of code length for (a) SSC and (b) GCC deployments.

with respect to the previous value. Accordingly, the results illustrated in Figure 8(b) verifies this criterion where we can see the SNIR for both sensors start from 0 dB at 4 bits case, increases by around 1.5 dB with respect to each increase in the code-length, reaching its maximum of nearly 6 dB at 64 bits.

V. DISCUSSION

The previous section has clearly explained the performance of simplex and Golay coded TDM-FBG sensors over the conventional single pulse technique. The two pulse coding techniques showed similar performance in the context of conserving the original spatial properties of the system. At all code lengths applied to both techniques, FBG pulses found to be identical to the original single pulse case, with slight advantages of the SSC deployment regarding the pulse shaping. The results also characterized the SSC by their denoising abilities, and the GCCs by their higher signal amplitude and extracting small signals amplitudes out of high noise background. Compared to the conventional single pulse case, the noise amplitude of the FBG pulses decoded over the 63 bits of SSC has been reduced by 31.5 times. In terms of signal amplitude, the peak amplitude of the FBG pulses decoded over the 64 bits of GCC has been amplified by 127.4 times. This context well explains the SNIR similarity between the two techniques although their noise and peak amplitudes behave differently. The high noise reduction provided to the system by the deployment of SSC guarantees the FBG signals with high SNR despite their weak amplitudes. Consecutively, the large peak FBG signals decoded over the GCC gains high SNR despite their high noise.

The final feature to be listed in this comparison is the processing time and the ease of use. For instance, achieving the SNIR value of 6 dB is possible whether by the deployment of 63 bits SSC or 64 bits GCC. However, it takes the SSC to launch and retrieve the total number of 63 times domain traces to achieve the targeted SNIR and doubling this number to achieve higher values. In contrast, it takes the GCC deployment 4 traces contains on all the 64 bits needed to achieve the same value of the targeted SNIR.

VI. CONCLUSIONS

In this work, the experimental deployment of two pulse coding techniques, standard simplex- (SSC) and Golay complementary codes (GCC) in the TDM-FBG sensor along a 16.35 km of fiber was successfully demonstrated. The interrogation scheme of SSC and GCC were individually analyzed and compared with that of conventional single pulse technique. We have confirmed that the deployment of simplex- and Golay codes in TDM-FBG sensor could improve the overall system performance without impairing the system spatial resolution. For all code lengths applied to both techniques, FBG decoded pulses found to be spatially identical to the conventional single pulse technique, with uniform raising and falling edges, confirming the correctness of Hadamard transform and Golay autocorrelation calculations.

Furthermore, we extensively studied the noise behavior and the amplitude of the decoded pulses for both coding techniques. The analysis confirmed that the SSC deployment resulted in well-formed pulses and excellent background noise, while the GCC deployment produced large amplitude of FBG signal. In an excellent agreement with the theory, the improvement of the performance parameters with the code length has also been confirmed. In details, compared to the conventional single pulse case, FBG pulses decoded at the codelengths of 63 bits SSC have shown lower noise by 31.5 times, while the 64 bits GCC have shown higher amplitude by 127.4 times. Despite the difference in the signal amplitude and noise behaviors, similar SNIR results have been obtained for both coding techniques. In the case of SSC, even though the signal amplitude did not increase with the code length, the decrease in the random noise due to longer code length has contributed to the SNR improvement. As for the GCC, the increase in signal amplitude due to longer code length has resulted in improved SNR, despite the simultaneous increase in the noise.

ACKNOWLEDGMENT

The authors would like to extend their gratitude towards UKM for allowing this research to be carried out and all supports that have been given throughout the process of this work. They would also like to extend their appreciation towards Photonics Technology Laboratory of Center of Advanced Electronic and Communication Engineering (PAKET), Faculty of Engineering and Built Environment, UKM for all the facilities provided.

REFERENCES

[1] R. Kashyap, *Fiber Bragg Gratings*. New York, NY, USA: Academic, 2009, p. 632.
[2] A. A. G. Abushagur, N. Arsad, M. I. Reaz, and A. A. A. Bakar, "Advances in bio-tactile sensors for minimally invasive surgery using the fibre Bragg grating force sensor technique: A survey," *Sensors*, vol. 14, no. 4, pp. 6633–6665, 2014.
[3] F. Jasmi, N. H. Azeman, A. A. A. Bakar, M. S. D. Zan, K. H. Badri, and M. S. Su'ait, "Ionic conductive polyurethane-graphene nanocomposite for performance enhancement of optical fiber Bragg grating temperature sensor," *IEEE Access*, vol. 6, no. 1, pp. 47355–47363, 2018.

[4] M. E. Haque, M. F. M. Zain, M. A. Hannan, M. Jamil, and H. Johari, "Recent application of structural civil health monitoring using WSN and FBG," *World Appl. Sci. J.*, vol. 20, no. 4, pp. 585–590, 2012.
[5] M. Majumder, T. K. Gangopadhyay, A. K. Chakraborty, K. Dasgupta, and D. K. Bhattacharya, "Fiber Bragg gratings in structural health monitoring-present status and applications," *Sens. Actuators A, Phys.*, vol. 147, no. 1, pp. 150–164, 2008.
[6] X. Wen, H. Shuai, F. Zhu, and D. Zhang, "Fiber Bragg gratings sensing network with a bus chain typology structure," *Opt. Eng.*, vol. 55, no. 6, pp. 066102-1–066102-5, 2016.
[7] Y. Wang, J. Gong, B. Dong, D. Y. Wang, T. J. Shillig, and A. Wang, "A large serial time-division multiplexed fiber Bragg grating sensor network," *J. Lightw. Technol.*, vol. 30, no. 17, pp. 2751–2756, Sep. 1, 2012.
[8] Y. Wang, J. Gong, D. Y. Wang, B. Dong, W. Bi, and A. Wang, "A quasi-distributed sensing network with time-division-multiplexed fiber Bragg gratings," *IEEE Photon. Technol. Lett.*, vol. 23, no. 2, pp. 70–72, Jan. 15, 2011.
[9] J. Liu, J. Zhang, X. Li, and Z. Zheng, "Study on multiplexing ability of identical fiber Bragg gratings in a single fiber," *Chin. J. Aeronaut.*, vol. 24, no. 5, pp. 607–612, 2011.
[10] C. C. Chan, Y. J. Gao, K. T. Lau, H. L. Ho, L. M. Zhou, and W. Jin, "Characterization of crosstalk of a TDM FBG sensor array using a laser source," *Opt. Laser Technol.*, vol. 33, no. 5, pp. 299–304, 2001.
[11] F. Zaidi, T. Nannipieri, A. Signorini, M. Taki, V. Donzella, and F. D. Pasquale, "High performance time domain FBG dynamic interrogation scheme based on pulse coding," *IEEE Photon. Technol. Lett.*, vol. 25, no. 5, pp. 460–463, Mar. 1, 2013.
[12] M. A. Soto, S. L. Floch, and L. Thévenaz, "Bipolar optical pulse coding for performance enhancement in BOTDA sensors," *Opt. Express*, vol. 21, no. 14, pp. 16390–16397, 2013.
[13] M. S. D. B. Zan and T. Horiguchi, "A dual golay complementary pair of sequences for improving the performance of phase-shift pulse BOTDA fiber sensor," *J. Lightw. Technol.*, vol. 30, no. 21, pp. 3338–3356, Nov. 1, 2012.
[14] M. S. D. Zan, A. A. A. Bakar, and T. Horiguchi, "Improvement of signal-to-noise-ratio by combining Walsh and Golay codes in modulating the pump light of phase-shift pulse BOTDA fiber sensor," in *Proc. 9th Int. Conf. Sens. Technol. (ICST)*, Auckland, New Zealand, Dec. 2015, pp. 269–273.
[15] M. M. Elgaud, M. S. D. Zan, A. G. Abushagur, and A. A. A. Bakar, "Improvement of signal to noise ratio of time domain mutliplexing fiber Bragg grating sensor network with Golay complementary codes," *Opt. Fiber Technol.*, vol. 36, pp. 447–453, Jul. 2017.
[16] N. Park *et al.*, "Coded optical time domain reflectometry: Principle and applications," *Proc. SPIE*, vol. 6781, p. 678129, Nov. 2007.
[17] M. D. Jones, "Using simplex codes to improve OTDR sensitivity," *IEEE Photon. Technol. Lett.*, vol. 5, no. 7, pp. 822–824, Jul. 1993.
[18] M. Golay, "Complementary series," *IRE Trans. Inf. Theory*, vol. 7, no. 2, pp. 82–87, Apr. 1961.
[19] M. Nazarathy *et al.*, "Real-time long range complementary correlation optical time domain reflectometer," *J. Lightw. Technol.*, vol. 7, no. 1, pp. 24–38, Jan. 1989.
[20] C. G. Wallace, A. E. Kelly, D. Uttamchandani, and I. Andonovic, "New unipolar codes allowing electrooptical correlation utilizing a semiconductor laser amplifier," *IEEE Photon. Technol. Lett.*, vol. 7, no. 12, pp. 1456–1458, Dec. 1995.

M. M. ELGAUD received the B.E. degree in electrical and electronic engineering from Benghazi University Benghazi, Libya, in 2005, and the M.Sc. degree in telecommunication and computer science from Universiti Kebangsaan Malaysia in 2011, where he is currently pursuing the Ph.D. degree in fiber Bragg grating (FBG) sensors and its applications in distributed optical fiber networks. His current work focuses on signal processing methods to improve the performance of time-domain multiplexed FBG sensor arrays.

AHMAD ASHRIF A. BAKAR (M'02–SM'12) received the bachelor's degree in electrical and electronics engineering from Universiti Tenaga Nasional in 2002, the M.Sc. degree in communications and network system engineering from Universiti Putra Malaysia in 2004, and the Ph.D. degree in electrical engineering from The University of Queensland, Australia, in 2010. He is currently an Associate Professor with the Center of Advanced Electronic and Communication Engineering, Faculty of Engineering and Built Environment, Universiti Kebangsaan Malaysia. He is actively involved in the Optical Society of America and Fiber Optic Association Inc., USA. He is devoting his research work on optical sensors in environmental and biomedical application, specialized in plasmonic waveguide sensor, polymeric electro-optic modulator waveguide, interferometer, evanescent field sensors, and devices based on nanoparticles and nanostructures. He has been a member of OSA since 2014.

ABDULFATAH ABUSHAGUR GHAITH received the B.E. degree in electrical engineering from the Higher Institute of Mechanical/Electrical Engineering, Hun, Libya, in 1992, and the M.Sc. and Ph.D. degrees in electrical, electronic and systems engineering from Universiti Kebangsaan Malaysia in 2012 and 2018, respectively. He is currently a Research Officer with the Photonics Technology Laboratory, Center of Advanced Electronic and Communication Engineering, Faculty of Engineering and Built Environment, Universiti Kebangsaan Malaysia. His current research interest is in the optical fiber sensors, focusing on fiber Bragg grating sensors and its applications in biomedical engineering.

NANI FADZLINA NAIM received the B.Eng. degree in electrical and electronics engineering and the M.Eng. degree in electronics and communication engineering and the Ph.D. degree in electrical, electronics and systems engineering from Universiti Teknologi Malaysia in 2005, 2007, and 2015, respectively. Her current research interests are in the area of photonic networks, and optical sensing technology and its application.

NORHANA ARSAD (M'10) received the B.Eng. degree in computer and communication systems and the M.Sc. degree in photonics from Universiti Putra Malaysia, Malaysia, in 2000 and 2003, respectively, the Ph.D. degree from the University of Strathclyde, Glasgow, U.K., in 2010. She is currently an Associate Professor with the Center of Advanced Electronic and Communication Engineering, Faculty of Engineering and Built Environment, Universiti Kebangsaan Malaysia. Her research interest is in the investigation and design of fiber laser systems for application in spectroscopy, gas sensing, and photonics technology.

MOHD HADRI HAFIZ MOKHTAR (M'18) received the M.Eng. degree in electrical and electronics from the University of Birmingham, U.K., in 2009, and the Ph.D. degree in electrical engineering from the Imperial College London in 2016. He is currently a Senior Lecturer with the Center of Advanced Electronic and Communication Engineering, Faculty of Engineering and Built Environment, Universiti Kebangsaan Malaysia. His research interest is in fiber-based optical imaging and optical sensors and its applications.

NUR HIDAYAH AZEMAN received the B.Sc. degree in resource chemistry from Universiti Malaysia Sarawak in 2009 and the Master of Environment and Ph.D. degrees in smart sensing materials from Universiti Putra Malaysia in 2012 and 2017, respectively. She is currently a Post-Doctoral Researcher with the Center of Advanced Electronic and Communication Engineering, Faculty of Engineering and Built Environment, Universiti Kebangsaan Malaysia, with a focus on the development of optical fiber sensor for environmental monitoring. Her research interests include functional materials, and optical fiber sensors and its applications.

MOHD SAIFUL DZULKEFLY ZAN (M'15) received the bachelor's degree in electronics, information, and communication engineering from Waseda University, Japan, in 2006, the master's and Ph.D. degrees from the Shibaura Institute of Technology, Japan, in 2011 and 2014, respectively. During his Ph.D. study, he proposed the optical pulse coding technique to improve the sensing performance of Brillouin optical time-domain analysis (BOTDA) fiber-optic sensor. He is currently a Senior Lecturer with Universiti Kebangsaan Malaysia. His research interests involve Brillouin scattering-based fiber-optic sensor, such as BOTDA, BOTDR, optical pulse coding technique for fiber sensors, and Brillouin scattering-based fiber laser. He is also conducting research on fiber Bragg grating sensor.